

# Effect of Halloysite Nanoclay on Polymerization and Properties of Poly(3,4-(2,2-dimethylpropylenedioxy) - thiophene-*co*-aniline)

Ayesha Kausar

Nanosciences and Catalysis Division, National Centre For Physics, Quaid-i-Azam University Campus, Islamabad, Pakistan

**Abstract** In the present work, poly(3,4-(2,2-dimethylpropylenedioxy)thiophene-*co*-aniline) was prepared through *in-situ* polymerization of 3,4-(2,2-dimethylpropylenedioxy)thiophene and aniline (PDMPT-*co*-PANI/Halloysite). Later, halloysite nanoclay reinforced PDMPT-*co*-PANI composites has been prepared and their thermal stability and flammability were investigated. Molecular weight of *in-situ* polymerized PDMPT-*co*-PANI copolymer was found to decrease according to gel-permeation chromatography. The PDMPT-*co*-PANI/Halloysite composites were nanodispersed with layered morphology according to FESEM analysis. They composites exhibited higher heat stability and considerably reduced peak heat release rate with the halloysite nanoclay addition. The reasons were the formation of ceramic char layer over the composite surface during combustion and physico-chemical adsorption of volatile products on silicate surface. The addition of nanoclay formed inorganic-rich surface leading to enhanced thermal stability and reduced flammability of the composites.

**Keywords** Halloysite, *In-situ* polymerization, Gel-permeation chromatography, Thermal stability, Flammability.

## 1. Introduction

In the field of conductive polymers, incessant technological developments have directed towards new applications. A range of conjugated polymers having fine physical properties have been developed. The improved properties of conjugated polymers are their fine processibility, electrical properties, and thermal stability [1]. In order to attain fine material properties molecular structure of organic backbone can be tailored. Structural alterations have rendered these polymers important in sensor protection, optical computing, and optical wave guide devices [2]. One of the methods for improving the processibility of conjugated polymers is the copolymerization with some solvent miscible fragments. The properties of copolymerized material such as toluidine and anisidine depend on the type of substitution. Studies have demonstrated that the electron withdrawing group decreases the electron density on aromatic ring (aniline) while electron donating group increases the electron density on the ring [3]. Consequently, the formation of poly(aniline-*co*-*m*-nitroaniline) (a copolymer of aniline with *m*-nitroaniline) has been reported by chemical and electrochemical polymerization [4].

Flame retardancy of polymeric materials has been

improved using a number of polymer additives. Usually, conventional fillers are not efficient flame retardants and the physical properties of polymers are inadequately affected by the addition of fillers. Initially, halogenated (bromine and chlorine), phosphorus-containing, inorganic, and melamine flame retardants have been explored. Among these flame retardants, inorganic fillers are non-hazardous and may not deteriorate the materials properties. Nanoadditives are also an important category of flame retardants [5]. Commonly employed inorganic flame retardants are nanoclay [6], carbon nanotubes [7], graphene [8], and nanosilica [9]. Major roles of the inorganic nanoadditives comprise noteworthy advancement in the physical properties of polymer such as thermal stability, flame retardancy, oxidative stability, etc. When exposed to fire, nanoadditive form superb gas barrier, so deferring the oxidative degradation of resin. Furthermore, the larger surface area of nanoadditives might persuade larger char yield averting the heat exposure. However, the key impediments towards the efficacy of inorganic nanoadditive are the aggregation of nanoparticles and increase of resin viscosity at high loading levels [10-12]. Recently nanoclays have been extensively explored as flame retardants. Nanoclays are found to show decrease in peak heat release rate (PHRR), increase in char residue, and decrease in rate of mass loss during cone calorimetric experiments [13, 14]. Nanoclays also overcome the drawbacks shown by non-silicate additives. According to recent research, flame retardant mechanism involves the formation of carbonaceous silicate char over the composite

\* Corresponding author:

asheesgreat@yahoo.com (Ayesha Kausar)

Published online at <http://journal.sapub.org/ajps>

Copyright © 2015 Scientific & Academic Publishing. All Rights Reserved

surface thus insulating the underlying material [15]. Thermal stability and flammability of montmorillonite-based composite systems have been explored extensively [16, 17]. These nanocomposites may have lowest PHRR; although no noticeable decrease in PHRR values were observed [18]. Here we chose to study a copolymeric system of 3,4-(2,2-dimethylpropylene-dioxy)thiophene and aniline for two reasons. First, the thermal stability of rigid-rod materials would be expected high in accordance with polyaniline and polythiophene systems. Secondly, sulfur containing thiophene moiety may also contribute to flame retardance in addition to the nanoclay used.

## 2. Experimental

### 2.1. Materials

Halloysite nanoclay (nanopowder, nanotube diam. $\times$ L = 30-70 nm $\times$ 1-3  $\mu$ m; pore volume = 1.26-1.34 mL/g), 3,4-(2,2-dimethylpropylenedioxy)thiophene (97 %), aniline ( $\geq$  99.5 %), iron(III) chloride ( $\text{FeCl}_3$  reagent grade, 97 %), and hydrochloric acid (HCl, 37 %) were obtained from Aldrich.

### 2.2. Characterization

The number average and weight-average molecular weight ( $M_w$ ) were measured using Viscotek TDAmx. Field Emission Scanning Electron Microscopy (FE-SEM) of freeze fractured samples was performed using JSM5910, JEOL Japan. Thermal stability was verified by METTLER TOLEDO TGA/DTA thermo gravimetric analyzer using 3 mg of the sample in  $\text{Al}_2\text{O}_3$  crucible at a heating rate of 10  $^\circ\text{C}/\text{min}$ . The combustion properties of nanocomposites were calculated using cone calorimetry. Samples having dimensions 100  $\times$  100  $\times$  5 mm<sup>3</sup> were exposed to a FTT 0007 cone calorimeter (FTT Company, England) under a heat flux of 50 kW/m<sup>2</sup> according to ISO-5660 standard procedure. Typical results from cone calorimeter reported here were the averages of triplicate.

### 2.3. Functionalization of Halloysite Nanoclay

The aminopropyl-functionalized halloysite nanoclay was prepared by adding 3-aminopropyltriethoxysilane (10 mL) to an ethanolic solution of halloysite nanoclay (1 g) in ethanol (20 mL). After 2 h, the slurry obtained was stirred overnight, and then the precipitate was collected after centrifugation. The precipitate was washed with absolute ethanol and dried at 60  $^\circ\text{C}$ .

### 2.4. Preparation of poly(3,4-(2,2-dimethylpropylenedioxy)thiophene-co-aniline) (PDMPT-co-PANI)

For polymerization, 3,4-(2,2-dimethylpropylenedioxy)thiophene (0.5 mL) was added in 0.1 M HCl (50 mL) and

sonicated for 12 h. To the above solution, 50 mL of  $\text{FeCl}_3/\text{HCl}$  solution (1.2 g  $\text{FeCl}_3/0.1$  M HCl) was added drop wise. Afterwards, a 50 mL solution of aniline (0.5 mL) and 0.1 M HCl was prepared and added slowly to the above mixture. The mixture was further agitated for 12 h resulting in the co-polymerization of aniline and thiophene-based monomer. The sample was filtered, washed (water/ethanol) and dried to obtain PDMPT-co-PANI powder [19].

### 2.5. Preparation of PDMPT-co-PANI/ Halloysite Composites

The PDMPT-co-PANI/Halloysite composite, in the proportions of 1, 3, 5 and 10 % of nanoclay were prepared *via in-situ* polymerization of 3,4-(2,2-dimethylpropylenedioxy)thiophene and aniline. Initially, the solution containing aniline (0.5 mL), 3,4-(2,2-dimethylpropylenedioxy)thiophene (0.5 mL) and  $\text{FeCl}_3/\text{HCl}$  solution (50 mL) along with the desired amount of clay was refluxed for 24 h at 60  $^\circ\text{C}$ . The composite obtained was filtered (cellular membrane filter paper) and washed several times with water and ethanol to remove the residual oxidant. Finally, the product was dried at 60  $^\circ\text{C}$  for 6 h. FTIR (KBr,  $\text{cm}^{-1}$ ): 3403 (O-H stretch), 3378 (N-H stretch), 1596 (N-H bend), 2999 (Ar C-H stretch), 2909 (Aliph C-H stretch), 1413 (C-N), 1233 (C-O), 1050 (C-S).

## 3. Results and Discussion

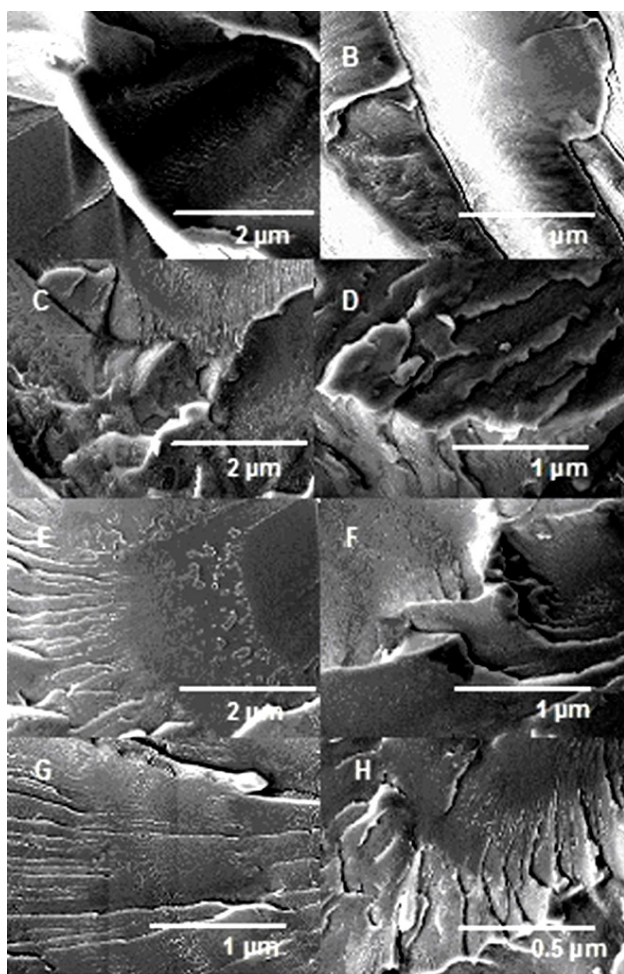
### 3.1. Effect of Nanoclay Addition on Molecular Weight

Gel-permeation chromatography was used to study the effect of nanoclay addition on molecular weight of PDMPT-co-PANI copolymer (Table 1). Addition of nanoclay during the *in-situ* copolymerization of PDMPT-co-PANI was studied using dilute samples. The presence of filler was expected to decrease the molecular weight of the copolymer. The  $M_n$  and  $M_w$  of copolymer were found to be  $19 \times 10^3$  and  $25 \times 10^3$  and  $\text{gmol}^{-1}$  respectively. In PDMPT-co-PANI/Halloysite 1 with 1 wt. % nanoclay, the number average and weight average molecular weights were decreased to 18 and  $22 \times 10^3$   $\text{gmol}^{-1}$  respectively. For PDMPT-co-PANI/Halloysite 3 having 3 wt. % filler content, the molecular weight values were further decreased to 15 and  $19 \times 10^3$   $\text{gmol}^{-1}$  respectively. Similarly, PDMPT-co-PANI/Halloysite 5 revealed more decline in the property to  $M_n = 12$   $\text{gmol}^{-1}$  and  $M_w = 17$   $\text{gmol}^{-1}$ . With 10 wt. % filler content, the number average molecular weight reached the value of  $9 \times 10^3$   $\text{gmol}^{-1}$ , while the weight average molecular weight decreased to  $11 \times 10^3$   $\text{gmol}^{-1}$  in PDMPT-co-PANI/Halloysite 10. Nevertheless, the values were fairly higher to represent reasonable molecular weight. Briefly, the adding up of nanoclay deficiently affected the copolymerization of PDMPT and PANI during *in-situ* process.

**Table 1.** Effect of Halloysite loading on molecular weight of *in-situ* polymerized PDMPT-co-PANI

| Sample                      | Nanoclay content | $M_n \times 10^3$ (gmol <sup>-1</sup> ) | $M_w \times 10^3$ (gmol <sup>-1</sup> ) | PDI ( $M_w/M_n$ ) |
|-----------------------------|------------------|---|---|-------------------|
| PDMPT-co-PANI               | 0                | 19                                      | 25                                      | 1.3               |
| PDMPT-co-PANI/Halloysite 1  | 1                | 18                                      | 22                                      | 1.2               |
| PDMPT-co-PANI/Halloysite 3  | 3                | 15                                      | 19                                      | 1.3               |
| PDMPT-co-PANI/Halloysite 5  | 5                | 12                                      | 17                                      | 1.4               |
| PDMPT-co-PANI/Halloysite 10 | 10               | 9                                       | 11                                      | 1.2               |

### 3.2. Morphology of PDMPT-co-PANI/ Halloysite Composites



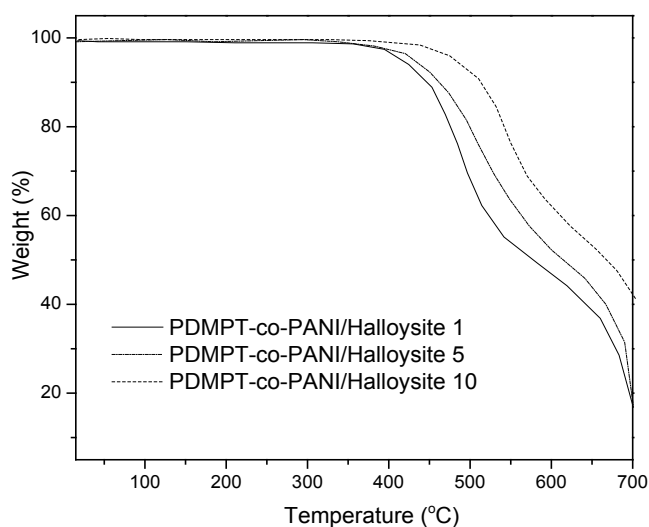
**Figure 1.** FESEM images of (A) PDMPT-co-PANI/Halloysite 1 at 2  $\mu\text{m}$ ; (B) PDMPT-co-PANI/Halloysite 1 at 1  $\mu\text{m}$ ; (C) PDMPT-co-PANI/Halloysite 3 at 2  $\mu\text{m}$ ; (D) PDMPT-co-PANI/Halloysite 3 at 1  $\mu\text{m}$ ; (E) PDMPT-co-PANI/Halloysite 5 at 2  $\mu\text{m}$ ; (F) PDMPT-co-PANI/Halloysite 5 at 1  $\mu\text{m}$ ; (G) PDMPT-co-PANI/Halloysite 10 at 1  $\mu\text{m}$ ; (H) PDMPT-co-PANI/Halloysite 10 at 0.5  $\mu\text{m}$

Fig. 1 shows the dispersion state of composites observed by FESEM images of fractured surfaces of PDMPT-co-PANI/Halloysite. The fractured surfaces of PDMPT-co-PANI/Halloysite 1 (Fig. 1A & B) seem to be

smooth and showed some signs of plastic flowing corresponding to brittle failure of homogenous material. Differing from the fractured surface of 1 wt. % loaded clay composite, the fractured surface of PDMPT-co-PANI/Halloysite 3 revealed indication of less plastic deformation having layered surface and rough fractured pieces (Fig. 1C & D). This type of morphology corresponds to improved toughness owing to the existence of layered silicate structure in matrix. However, the morphology of PDMPT-co-PANI in the presence of 5 wt. % nanoclay was changed. Fig. 1E & F showed relatively fine layering of matrix and nanoclay in PDMPT-co-PANI/Halloysite 5. The morphology has shown that there existed optimal concentration (5 wt. % nanoclay) for better dispersion of nanofiller in the matrix. Similarly, PDMPT-co-PANI/Halloysite 10 has shown uniform layering of the copolymer matrix and uniform dispersion of the clay particles (Fig. 1G & H). With the increasing clay content, PDMPT-co-PANI and halloysite nanoclay layers were found to be closely stacked compared with the 1 wt % of the nanofiller composite.

### 3.3. Thermogravimetric Analysis

Thermogravimetric analysis (TGA) was used to examine the effect of halloysite nanoclay addition on the thermal stability of PDMPT-co-PANI copolymer matrix. Fig. 2 shows the weight loss of pristine copolymer, PDMPT-co-PANI/Halloysite 1, PDMPT-co-PANI/Halloysite 3, and PDMPT-co-PANI/Halloysite 5 composites. Neat copolymer had initial degradation temperature ( $T_0$ ) of 355  $^{\circ}\text{C}$ , 10 % degradation temperature ( $T_{10}$ ) of 379  $^{\circ}\text{C}$  and maximum degradation temperature ( $T_{\text{max}}$ ) of 399  $^{\circ}\text{C}$  respectively. As can be seen from thermograms that there is a clear difference in the thermogravimetric curves of 1 and 10 wt. % nanoclay loaded composites. PDMPT-co-PANI / Halloysite 1 had  $T_0$ ,  $T_{10}$  and  $T_{\text{max}}$  of 420, 432 and 521  $^{\circ}\text{C}$  respectively. PDMPT-co-PANI/Halloysite 5 showed higher values of  $T_0$ ,  $T_{10}$  and  $T_{\text{max}}$  of 468, 479 and 567  $^{\circ}\text{C}$  respectively. The thermal stability of PDMPT-co-PANI / Halloysite 10 was further increased to 587  $^{\circ}\text{C}$  for maximum degradation temperature. The thermal stability of the composites was found to be higher than the literature clay materials [20, 21].



**Figure 2.** Thermogravimetric analysis of PDMPT-*co*-PANI/Halloysite composites

**Table 2.** Thermal analysis data of PDMPT-*co*-PANI/Halloysite composites

| Composition                          | T <sub>0</sub> (°C) | T <sub>10</sub> (°C) | T <sub>max</sub> (°C) |
|--------------------------------------|---------------------|----------------------|-----------------------|
| PDMPT- <i>co</i> -PANI               | 355                 | 379                  | 399                   |
| PDMPT- <i>co</i> -PANI/Halloysite 1  | 420                 | 432                  | 521                   |
| PDMPT- <i>co</i> -PANI/Halloysite 3  | 434                 | 443                  | 533                   |
| PDMPT- <i>co</i> -PANI/Halloysite 5  | 468                 | 479                  | 567                   |
| PDMPT- <i>co</i> -PANI/Halloysite 10 | 511                 | 527                  | 587                   |

### 3.4. Flame Retardancy of PDMPT-*co*-PANI/Halloysite Composites

In order to investigate the flame retardancy, cone calorimetry technique was used. Fig. 3 shows overlay plots of heat release rate (HRR) versus time for PDMPT-*co*-PANI/Halloysite composites; the corresponding data are summarized in Table 3. As for PDMPT-*co*-PANI/Halloysite 1 composite, the maximum peak (PHRR) (370 kW/m<sup>2</sup>) displays 5 % decrease with respect to PDMPT-*co*-PANI (390 kW/m<sup>2</sup>). However, with respect to PDMPT-*co*-PANI/Halloysite composites, it can be seen that all the composites have almost comparable length of igniting time to peak HRR. PDMPT-*co*-PANI/Halloysite 3 composite, displayed 13 % reduction (325 kW/m<sup>2</sup>) in PHRR compared with PDMPT-*co*-PANI/Halloysite 1. There was further decrease in the peak heat release rate for PDMPT-*co*-PANI/Halloysite 5 composite (280 kW/m<sup>2</sup>). PDMPT-*co*-PANI/Halloysite 10 composite had HRR of 238 kW/m<sup>2</sup> i.e. 36 % lower than PDMPT-*co*-PANI/Halloysite 1. The heat release rate of composites during combustion indicated that the nanoclay has significantly slowed down the combustion process and have shown better flame retardancy. The higher halloysite content was therefore more effective. The flammability of the composites was found comparable to the reported materials [20, 22, 23].

**Table 3.** Cone calorimeter data for PDMPT-*co*-PANI/Halloysite composites

| Sample                               | PHRR (kW/m <sup>2</sup> ) | Time to PHRR (s) |
|--------------------------------------|---------------------------|------------------|
| PDMPT- <i>co</i> -PANI               | 390                       | 157              |
| PDMPT- <i>co</i> -PANI/Halloysite 1  | 370                       | 153              |
| PDMPT- <i>co</i> -PANI/Halloysite 3  | 325                       | 151              |
| PDMPT- <i>co</i> -PANI/Halloysite 5  | 280                       | 149              |
| PDMPT- <i>co</i> -PANI/Halloysite 10 | 238                       | 144              |

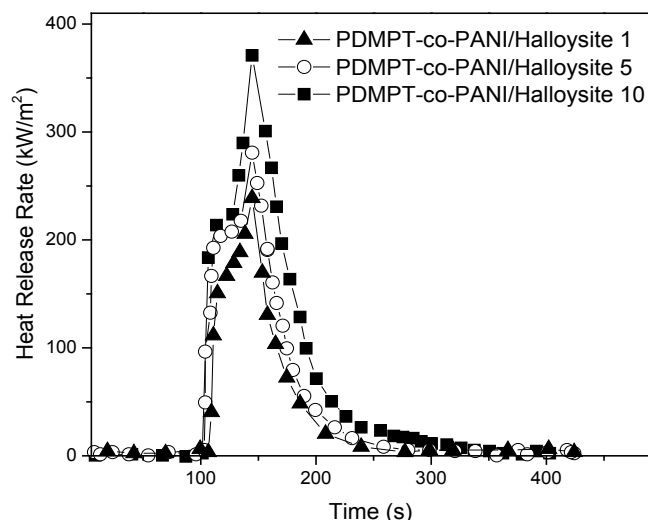


**Figure 3.** Dependence of heat release rate on time of PDMPT-*co*-PANI/Halloysite composites

## 4. Conclusions

In this work, a novel copolymer poly(3,4-(2,2-dimethylpropylenedioxy)thiophene-*co*-aniline) was prepared through *in-situ* polymerization and reinforced with halloysite nanoclay in various content. Effect of nanoclay addition on the number average and weight average molecular weight of copolymer revealed that the addition of filler hindered the copolymer chain growth. Later the morphology, thermal stability and flammability have been investigated. The addition of halloysite considerably increased the decomposition temperature of the matrix and reduced the PHRR of combustion. This was not only due to the barrier effect, but also because of the physico-chemical adsorption of the volatile degradation products on the nanoclay. TGA thermograms of the composite samples showed that the addition of nanoclay increased the initial and maximum decomposition of PDMPT-*co*-PANI/Halloysite under nitrogen. The HRR plots showed that the nanoclay inclusion reduced the ignition of copolymer matrix. It was observed that a compact char layer was formed on the surface of PDMPT-*co*-PANI/Halloysite composite during the combustion test. This was an important factor to increase the flame retardancy of these composites.

## REFERENCES

- [1] Dou L., You J., Yang J., Chen C. C., He Y., Murase S., Moriarty T., Emery K., Li G., Yang, Y., 2012, Tandem polymer solar cells featuring a spectrally matched low-bandgap polymer. *Nature Photonics*, 6(3), 180-185.
- [2] Chmielak B., Waldow M., Matheisen C., Ripperda C., Bolten J., Wahlbrink T., Nagel M., Merget F., Kurz H., 2011, Pockels effect based fully integrated, strained silicon electro-optic modulator. *Optics Express*, 19(18), 17212-17219.
- [3] Jaymand M., 2013, Recent progress in chemical modification of polyaniline. *Prog. Polym. Sci.*, 38(9), 1287-1306.
- [4] Ding L., Li Q., Zhou D., Cui H., Tang R., Zhai J., 2012, Copolymerization of aniline with m-nitroaniline and removal of m-nitroaniline from aqueous solutions using a polyaniline-modified electrode: A comparative study. *Electrochimica Acta*, 77, 302-308.
- [5] Isitman N. A., Dogan M., Bayramli E., Kaynak C., 2012, The role of nanoparticle geometry in flame retardancy of polylactide nanocomposites containing aluminium phosphinate. *Polym. Degrad. Stab.*, 97(8), 1285-1296.
- [6] Ghanbari A., Heuzey M. C., Carreau P. J., Ton-That M.T., 2013, A novel approach to control thermal degradation of PET/organoclay nanocomposites and improve clay exfoliation. *Polymer*, 54(4), 1361-1369.
- [7] Sattar R., Kausar A., Siddiq M., 2014, Advances in thermoplastic polyurethane composites reinforced with carbon nanotubes and carbon nanofibers: A review. *J. Plast. Film Sheet.*, DOI: 10.1177/8756087914535126.
- [8] Tang G., Jiang Z.-G., Lia X., Zhang H.-B., Hong S., Yua Z. Z., 2014, Electrically conductive rubbery epoxy/diamine-functionalized graphene nanocomposites with improved mechanical properties. *Compos. B Engineer.*, 67, 564-570.
- [9] Chiu Y., Tsai H., Imae T., 2012, Thermal and morphology properties of various silica contents in sulfone epoxy nanocomposites. *J. Appl. Polym. Sci.*, 125(1), 523-531.
- [10] Tai Q., Yuen R. K. K., Yang W., Qiao Z., Song L., Hu Y., 2012, Iron-montmorillonite and zinc borate as synergistic agents in flame-retardant glass fiber reinforced polyamide 6 composites in combination with melamine polyphosphate. *Composites A*, 43(3), 415-422.
- [11] Deka B. K., Maji T. K., 2012, Effect of silica nanopowder on the properties of wood flour/polymer composite. *Polym. Engineer. Sci.*, 52(7), 1516-1523.
- [12] Bharath K.N., Basavarajappa S., 2014, Flammability Characteristics of Chemical Treated Woven Natural Fabric Reinforced Phenol Formaldehyde Composites. *Procedia Mater. Sci.*, 5, 1880-1886.
- [13] Didane N., Giraud S., Devaux E., Lemort G., Capone G., 2012, Thermal and fire resistance of fibrous materials made by PET containing flame retardant agents. *Polym. Degrad. Stab.*, 97(12), 2545-2551.
- [14] Kuila T., Mishra A. K., Khanra P., Kim N. H., Lee J. H., 2013, Recent advances in the efficient reduction of graphene oxide and its application as energy storage electrode materials. *Nanoscale*, 5, 52-71.
- [15] Das P., Schipmann S., Malho J. -M., Zhu B., Klemradt U., Walther A., 2013, Facile Access to Large-Scale, Self-Assembled, Nacre-Inspired, High-Performance Materials with Tunable Nanoscale Periodicities. *ACS Appl. Mater. Interfaces*, 5 (9), 3738-3747.
- [16] Feyzi A., Faghihi K., Zolanvari A. A., 2013, Synthesis and Characterization of New Polyimide/Organoclay Nanocomposites Derived From 3,3',4,4'-Biphenyltetracarboxylic Dianhydride and 1, 2-Bis(4-Aminophenoxy)Ethane. *High Temp. Mat. Pro.*, 32(2), 171-178.
- [17] Chen J., Gao X., 2014, Review on the Fundamentals of Polymer Combustion and Flammability Characteristics for Hybrid Propulsion. *J. Polym. Biopolym. Phys. Chem.*, 2(4), 78-83.
- [18] Qin H. L., Su Q. S., Zhang S. M., Zhao B., Yang M. S., 2003, Thermal stability and flammability of polyamide 66/montmorillonite nanocomposites. *Polymer*, 44(24), 7533-7538.
- [19] Hussain S. T., Abbas F., Kausar A., Khan M. R., 2013, New polyaniline/polypyrrole/polythiophene and functionalized multi-walled carbon nanotubes based nanocomposites: Layer by layer in-situ polymerization. *High Perform. Polym.*, 25(1), 70-78.
- [20] Qina, H., Zhanga, S., Zhaoa, C., Fenga, M., Yanga, M., Shub, Z., Yang, S., 2004, Thermal stability and flammability of polypropylene/montmorillonite composites. *Polym. Degrad. Stab.*, 85(2), 807-813.
- [21] Ma, Z. L., Zhang, W. Y., Liu, X. Y., 2006, Using PA6 as a charring agent in intumescent polypropylene formulations based on carboxylated polypropylene compatibilizer and nano-montmorillonite synergistic agent. *J. Appl. Polym. Sci.*, 101(1), 739-746.
- [22] Tsoi, M., Zhuge, J., Chen R. -H., Gou, J., 2014, Modeling and experimental studies of thermal degradation of glass fiber reinforced polymer composites. *Fire Mater.*, 38(2), 247-263.
- [23] Zanetti, M., Kashiwagi, T., Falqui, L., Camino, G., 2002, Cone Calorimeter Combustion and Gasification Studies of Polymer Layered Silicate Nanocomposites. *Chem. Mater.*, 14(2), 881-887.